



# Bedrock-Hosted Diffusive Hot Storage for Large-Scale Thermo-Electric Energy Storage by Thermal Doublet

Denis Nguyen, Edoardo Gino Macchi, Catherine Colin, Nicolas Tauveron,  
Thomas Tartière

## ► To cite this version:

Denis Nguyen, Edoardo Gino Macchi, Catherine Colin, Nicolas Tauveron, Thomas Tartière. Bedrock-Hosted Diffusive Hot Storage for Large-Scale Thermo-Electric Energy Storage by Thermal Doublet. Procedia Engineering, 2017, 191, pp.1135-1143. 10.1016/j.proeng.2017.05.288 . hal-02915493

**HAL Id: hal-02915493**

**<https://brgm.hal.science/hal-02915493>**

Submitted on 6 Dec 2022

**HAL** is a multi-disciplinary open access archive for the deposit and dissemination of scientific research documents, whether they are published or not. The documents may come from teaching and research institutions in France or abroad, or from public or private research centers.

L'archive ouverte pluridisciplinaire **HAL**, est destinée au dépôt et à la diffusion de documents scientifiques de niveau recherche, publiés ou non, émanant des établissements d'enseignement et de recherche français ou étrangers, des laboratoires publics ou privés.

Symposium of the International Society for Rock Mechanics

## Bedrock-Hosted Diffusive Hot Storage for Large-Scale Thermo-Electric Energy Storage by Thermal Doublet

D. Nguyen<sup>a\*</sup>, E.G. Macchi<sup>b</sup>, C. Colin<sup>b</sup>, N. Tauveron<sup>c</sup>, T. Tartière<sup>d</sup>

<sup>a</sup> BRGM Languedoc-Roussillon, 1039 rue de Pinville, Montpellier 34000, France

<sup>b</sup> IMFT, Université de Toulouse, 2 Allée du Professeur Camille Soula, Toulouse 31400, France

<sup>c</sup> CEA, LITEN – DTBH/SBRT/LS2T, 17 rue des Martyrs, Grenoble 38054, France

<sup>d</sup> Enertime, 1 rue du Moulin des Bruyères, Courbevoie 92400, France

### Abstract

Superficial unfractured dry crystalline bedrock (e.g. granite) can constitute the diffusive hot storage for a large-scale thermo-electric energy storage by thermal doublet, an ice storage being the latent cold sink of the thermal doublet and supercritical CO<sub>2</sub> (sCO<sub>2</sub>) the heat transfer working fluid circulating inside closed-loop vertical geothermal exchangers. Operative 30°C–140°C thermal range of the diffusive hot storage will not alter mechanical resistance or thermal conductivity of the encasing bedrock. Technological issue for thermal coupling of the geothermal exchanger with the bedrock at working fluid temperatures above 100°C is solved by coaxial exchanger design implementing silicone rubber as wall material. Difficulties of modeling heat transfer for the full-scale geothermal exchanger due to Reynolds number up to 10<sup>6</sup> for the flow regime inside the exchanger are addressed through a simplified modeling approach. Experimental investigation on 1/10 scale heat exchanger prototype with sCO<sub>2</sub> as working fluid is conducted to study heat transfer performance and storage dynamics, and also to validate the full-scale modeling.

© 2017 The Authors. Published by Elsevier Ltd. This is an open access article under the CC BY-NC-ND license

(<http://creativecommons.org/licenses/by-nc-nd/4.0/>).

Peer-review under responsibility of the organizing committee of EUROCK 2017

**Keywords:** electricity storage; granite; modeling; heat transfer

### 1. Introduction

Massive integration of intermittent renewable energy production generates new challenges for the supervision and regulation of electric grids. The use of flexible but carbon-intensive technologies such as gas turbines has been the main solution in order to ensure the balance between demand and supply, maintaining grid frequency and power

\* Corresponding author. Tel.: +33(0)638656736 fax: +33(0)467645851.

E-mail address: [d.nguyen@brgm.fr](mailto:d.nguyen@brgm.fr)

quality. Large-scale electricity storage is an alternative with lower environmental impact. Pumped-Storage Hydroelectricity (PSH) accounts for more than 99% of the worldwide electricity storage bulk capacity, representing around 140 GW over 380 locations, and covers a power range varying from a few hundred of megawatts to a few gigawatts [1]. Despite having a long lifetime and being the most cost-effective energy storage technology, PSH requires construction of large water reservoirs, leading to high environmental impact. In addition, most suitable locations have already been used in developed countries. Compressed-Air Energy Storage (CAES) is at an advanced stage of development but accounts only two existing power plants because of an exceptional underground geological set-up needed for multi-megawatt energy storage. Thermo-electric energy storage (TEES) is an alternative that could provide large-scale electricity storage. Principle of TEES is as follows: during periods of excess electricity generation, a vapor compression heat pump consumes electricity and transfers heat between a low-temperature heat source and a higher temperature heat sink. The temperature difference between the heat sink and the heat source can be maintained for several hours, until a power cycle is used to discharge the system and generate electricity back to the grid during peak consumption. Mercangöz et al. [2] showed that the first study on TEES dates back to the 1920s, and described the general concept of this technology based on two-way conversion of electricity to and from heat. The authors analyzed a TEES system with CO<sub>2</sub> transcritical cycles, hot water and ice tanks as respectively hot and cold storage reservoirs. The ABB Corporate Research Center [3] described a way to store electricity using two hot water tanks, an ice tank and CO<sub>2</sub> transcritical cycles. Desrues et al. [4] studied a high temperature TEES system involving argon as working fluid following a closed thermodynamic Brayton cycle.

The purpose of the article is to present SeleCO2 project's concept [5] which implements ground storage as the diffusive hot storage for a large-scale thermo-electric energy storage by thermal doublet, an ice storage being the latent cold sink of the thermal doublet (Fig. 1). The design of the diffusive hot storage is addressed here from a geothermal point of view. Thermodynamic cycles' description for the thermo-electric energy storage operation, involving CO<sub>2</sub> transcritical heat-pump and power cycle, can be found in Ayachi et al. [5]. Section 2 of the article is devoted to the description of the ground diffusive hot storage, and addresses the high-temperature high-pressure geothermal heat exchanger technology that solves the technological issue of thermal coupling above 100°C between geothermal heat exchanger and encasing bedrock. Sections 3 and 4 are on thermal and mechanical simulations of the ground heat storage, and Section 5 on experimental measurements of thermo-physical properties after thermal cycling of samples of granite, a material which can be implemented as bedrock-hosted diffusive hot storage. Section 6 deals with modeling sCO<sub>2</sub> heat transfer with the encasing bedrock. Section 7 describes the experimental bench set up to investigate heat transfer performance and storage dynamics on a 1:10 scale heat exchanger prototype.

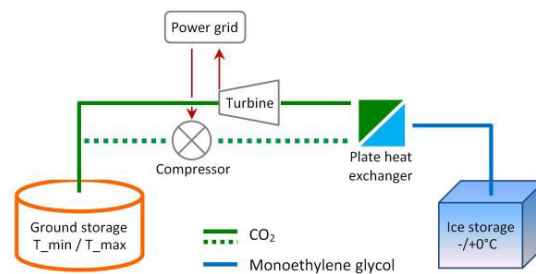


Fig. 1. Thermo-electric energy storage by thermal doublet “Ground hot storage + Ice cold storage”.

## 2. Description of the ground storage

### 2.1. Ground diffusive hot storage into unfractured dry crystalline bedrock

The ground heat storage (i.e. geostock) consists of several hundreds of short vertical coaxial geothermal heat exchangers (typically 12 m long, 200 mm diameter and 50 cm apart on hexagonal lay-out), set up on serial/parallel configuration into unfractured dry crystalline bedrock (e.g. granite). The shape of the geostock is a vertical cylinder with radius equal to height. This geometry minimizes the outer surface of the volume when the top side of

the geostock is thermally insulated (which is always possible), and thereby minimizes heat losses from the geostock to the environment. Fig. 2 shows 30° sector of a geostock assembling a total 48 lines parallel of 45 geothermal heat exchangers in series, that is 2160 exchangers. Thermal energy is transferred from/to the working fluid, circulating the closed-loop coaxial exchangers, to/from the encasing bedrock, respectively during storage charge/discharge. Temperature in the geostock is varying between 30°C and 140°C according to the charge/discharge multi-hours operating cycles. A site will not be suited for hosting the ground heat storage if there is underground water, as it will indicate fissured and altered bedrock, and might increase heat losses by underground water circulation.

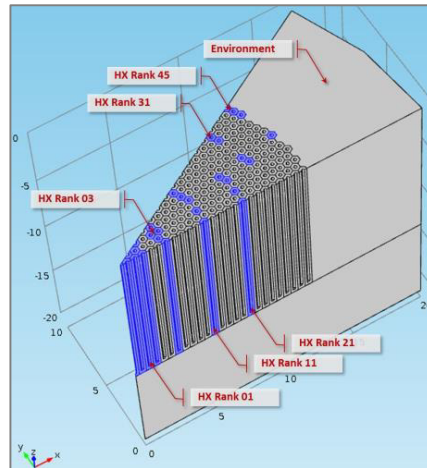


Fig. 2. 30° sector of the geostock showing for demonstration 4 parallel lines of 45 coaxial geothermal heat exchangers (HX) in series. Flow direction is from central to peripheral exchangers during storage charge of the geostock, and the opposite during storage discharge.

## 2.2. High-temperature high-pressure geothermal heat exchanger

In conventional geothermal operation with vertical geothermal probes, the boreholes are usually filled with a grout mix. The grout is a hydrated cement with high thermal conductivity that ensures the thermal coupling between the geothermal exchanger, in which the working fluid circulates, and the wall of the borehole and the surrounding rock mass. In the case of SeleCO<sub>2</sub> concept, the temperature of the working fluid in the geothermal exchangers can reach 140°C, which is incompatible with a grout. For temperatures higher than 100°C, shrinkage and cracking phenomena will occur in the hydrated cement resulting in separation of the grout from the geothermal exchanger wall, and induced thermal decoupling of the exchanger from the rock. Thermal coupling of the geothermal heat exchanger with the encasing bedrock for working fluid temperatures above 100°C clearly constitutes a technological issue for the concept of bedrock-hosted diffusive hot storage.

SeleCO<sub>2</sub> project solves the technological issue of thermal coupling above 100°C by a geothermal heat exchanger design implementing silicone rubber material for the wall of the 200 mm diameter coaxial exchanger. When under inside pressure of the working fluid, the exchanger outer wall will be pushed against the wall of the borehole, with no need for any grout. Enhanced thermal conductivity up to 3 W/(mK) is available for specialty silicone rubber and will guarantee adequate thermal coupling of geothermal exchanger with the rock. Material used for the coaxial exchanger inside tube is 0.3 W/(mK) standard silicone rubber. The silicone rubber exchanger design will also ease the containment of sCO<sub>2</sub> pressure that reaches 120 bar. Inside pressure in the exchanger is actually released against the encasing rock thanks to the silicone rubber elasticity of the exchanger outer wall. The top part of the geothermal exchanger, in contact with the ambient atmospheric pressure, has on the other hand to be held in place by a self-locking harness consisting of aramid straps. Experimental coefficient of friction  $\mu$  for an aramid strap under 120 bar compression between a sawn granite surface and a silicone rubber (60 shore A) sheet is measured and results to  $\mu = 0.24$ . The value demonstrates the feasibility of self-locking harness to hold in place the top part of the high-temperature high-pressure coaxial geothermal exchanger implementing silicone rubber as wall material.

### 3. Mechanical simulation for the bedrock diffusive hot storage

Due to the geothermal heat exchanger design, the pressure of the working fluid circulating inside the exchangers is fully released against the wall of the borehole. Coupled thermo-mechanical processes are only of a second-order of importance in the operating range of the storage. Mechanical simulations for the ground heat storage are performed by “Linear Elastic Material” model (Table 1). A maximum displacement of 1.7 mm is anticipated in the ground storage. Horizontal sections for von Mises stress evaluating a possible plastic flow (i.e. a non-reversible deformation) in the ground storage show no particular area of stress accumulation. Close to the heat exchangers, von Mises stress stays between 12 and 18 MPa and remains in the elastic range, well below the elastic limit of granite.

Table 1. Parameters for mechanical simulation of the ground heat storage by “Linear Elastic Material” model (COMSOL Multiphysics®).

| Parameters                     | Values   | Observation                             |
|--------------------------------|--|---|
| Geostock                       | 12.3 m radius – 12.3 m high  | Vertical cylinder                       |
| Environment                    | 25 m radius – 25 m high  | Zero displacement at boundaries limits  |
| Bedrock                        | 2650 kg/m <sup>3</sup> – Young's modulus 16 GPa – Poisson's ratio 0.26 | Unfractured dry granite                 |
| Coaxial geothermal exchangers  | 12 m long – 200 mm diameter – 50 cm axial inter-distance               | 2160 exchangers on hexagonal lay-out    |
| Pressure inside the exchangers | 120 bar (sCO <sub>2</sub> )  | Silicone rubber material for exchangers |

### 4. Thermal simulation for the bedrock diffusive hot storage

The diffusion of heat from the geostock towards the surrounding environment needs to be evaluated as it constitutes an energy loss for the storage system, and has a direct incidence on the electric storage efficiency of SeleCO<sub>2</sub> concept. Diffusive heat losses for the hot storage in its environment are evaluated considering the geostock as a whole. In other words, individual exchangers are here not considered to simplify the thermal simulation of the ground storage. (Further works are in process for a thermal geostock model considering individual heat exchangers).

Two situations for the entire geostock are hence simulated by “Heat Transfer in Solids” model (Table 2). Simulation A: at the beginning geostock temperature is 138°C with a 20°C surrounding environment; this could approach a situation of stand-by of the geostock between a charge and a discharge cycle with no circulation of sCO<sub>2</sub> inside the geothermal exchangers. Simulation B: succession over 800 h of thermal cycles of charge (duration 4 h, fluid inlet temperature in the exchangers at core: 138°C – Flow direction is from central to peripheral exchangers during charge and the opposite during discharge) and discharge (duration 8 h, fluid inlet temperature at periphery 30°C); this could represent typical operating case for the geostock. Noteworthy results of both simulations are as follows: for case A, 91% of the initial stored thermal energy (318 MWh) remains in the geostock after 80 h of operating stand-by (i.e. diffusive heat loss in the environment 9%); for case B, exergy efficiency of the storage is about 70%, and in some operative situations the environment can return leaked energy back to the geostock.

Table 2. Parameters for diffusive heat loss simulations of a ground heat storage by “Heat Transfer in Solids” model (COMSOL Multiphysics®).

| Parameters                 | Values  | Observation                             |
|----------------------------|---|---|
| Geostock                   | 12.3 m radius – 12.3 m high                         | Vertical cylinder                       |
| Environment                | 20 m radius – 20 m high                             | Zero heat transfer at boundaries limits |
| Bedrock                    | 2650 kg/m <sup>3</sup> – 790 J/(kg·K) – 3.4 W/(m·K) | Unfractured dry granite                 |
| Simulation A (80 h total)  | Geostock: 411 K - Environment: 293 K                | At t = 0 s                              |
| Simulation B (800 h total) | Geostock periphery during charge cycle: 323 K       | Duration of charge cycle: 4 h           |
|                            | Geostock periphery during discharge cycle: 303 K    | Duration of discharge cycle: 8 h        |
|                            | Geostock core: 411 K unchanged charge or discharge  | Radial linear thermal zonation          |
|                            | Environment: 293 K                                  | At t = 0 s (Start of thermal cycling)   |

## 5. Experimental acquisitions of mechanical and thermo-physical rock properties after thermal cycling

Impact of thermal cycling on mechanical and thermo-physical properties is investigated for Sénonès granite [6]. Mechanical behavior of this granite material was previously studied under static thermal condition up to 600°C by R. Houpert and Homand-Etienne [7]. Dimensions of cylindrical granite samples submitted to thermal cycling are 50 mm diameter and 150 mm height. Thermal conductivity ( $\lambda$ ) is measured by Hot Disk equipment, and compressive strength (Rc and  $\nu$ ) by uniaxial compressive test.

Results are confronted between samples, as a same sample can't be submitted to various total numbers of thermal cycles due to the destructive uniaxial compressive test performed after the thermal cycling. No evident relationship between number of cycles and uniaxial compressive strength, or between number of cycles and thermal conductivity, can be inferred on tested samples given the dispersion of compressive strength and thermal conductivity within samples batch (Table 3). Uniaxial compression strength and thermal conductivity of granite samples do not appear to change significantly after several hundred of thermal cycles between 30°C and 140°C. The experimental results reinforces the concept of diffusive hot storage in crystalline rocks, as operating conditions of the energy storage will not alter mechanical resistance or thermal conductivity of the encasing bedrock.

Table 3. Mechanical and thermo-physical experimental properties of Sénonès granite samples before and after thermal cycling.

| Granite sample ID | Number of thermal cycles<br>30°C–140°C<br>Gradient 1°C/min | Before thermal cycling         |                       | After thermal cycling |             |       |                        |   |
|-------------------|--|--------------------------------|-----------------------|-----------------------|-------------|-------|------------------------|---|
|                   |  | $\rho$<br>[kg/m <sup>3</sup> ] | Total porosity<br>[%] | Total porosity<br>[%] | Rc<br>[Mpa] | $\nu$ | $\lambda$<br>[W/(m·K)] | $\rho C_p$<br>[MJ/(mm <sup>3</sup> ·K)] |
| A                 | Zero cycle   | 2698                           | 1.11                  | -                     | 167.8       | 0.17  | 2.71                   | 2.05                                    |
| B                 | 100 cycles   | 2692                           | 0.77                  | 0.82                  | 136.4       | 0.17  | 2.45                   | 1.86                                    |
| C                 | 200 cycles   | 2690                           | 0.76                  | 0.93                  | 168.1       | 0.13  | 2.70                   | 1.91                                    |
| D                 | 300 cycles   | 2690                           | 0.72                  | 0.82                  | 158.9       | 0.18  | 2.49                   | 1.88                                    |
| E                 | 400 cycles   | 2687                           | 0.69                  | 0.74                  | 151.1       | 0.15  | 2.44                   | 1.82                                    |
| F                 | 500 cycles   | 2687                           | 0.60                  | 0.71                  | 159.0       | 0.15  | 2.69                   | 1.96                                    |
| G                 | 600 cycles   | 2687                           | 0.58                  | 0.67                  | 157.1       | 0.15  | 2.80                   | 1.94                                    |

## 6. Modeling sCO<sub>2</sub> heat transfer with the encasing bedrock

### 6.1. Difficulties and modeling approach: conjugate heat transfer CFD, 1D and 0D numerical models

The ground heat storage is the central part of this system, but it is also the most complex part to model. The main difficulties come from the particularly high Reynolds number in the exchangers (Re between 10<sup>5</sup> and 10<sup>6</sup>), the large size of the storage and the different time-scales of the process (from seconds, for the flow dynamics, to days, for the heat storage behavior during multiple charge/discharge cycles). A detailed conjugate heat transfer CFD study is viable only for a single exchanger and for very short durations.

Yet in order to optimize the storage system we need to model several multi-hours charge/discharge cycles considering at least a line of 45 exchangers in serie (which is representative of the behavior of the whole geostock). It's therefore evident that a simplified model for the thermo-fluid dynamic behavior of CO<sub>2</sub> inside the exchangers is required. Since an in-depth model validation will be not possible, we first decided to introduce only a geometrical simplification resorting to an unsteady 1D model for the fluid coupled with an unsteady 2D axisymmetric model for the heat transfer inside the rock [8]. It should be noted that in this “1D” model the interactions between the exchangers (i.e. heat conduction between the rock surrounding each exchanger) and the heat losses toward the rock surrounding the whole ground storage are assumed to be negligible. The former aspect can be neglected since the temperature difference between adjacent exchangers is small, while the latter aspect is important only during the start-up phase when the temperature of the rock that surrounds the ground storage is different from the temperature of the rock surrounding the peripheral exchangers. Also note that due to the intrinsic unsteadiness of

the heat storage system, it is fundamental to adopt an unsteady model for both fluid and rock. For reasons of high computational time the 1D model is however not really suited for modeling the whole ground heat storage while taking into account both the interactions between exchangers and the heat losses of the geostock into the environment.

An even simpler “0D” model, based on the solution of global mass and energy balances for each exchanger, has hence been developed for the purpose of modeling the whole ground heat storage. This 0D model, described in the next paragraphs, has been validated by comparison with the mentioned 1D model considering the same conditions for the rock (no heat losses and no interactions between exchangers). However the 0D model for the fluid can easily be coupled with any thermal model for the rock, thus allowing thermal simulation for real geometry of the whole ground heat storage considering individual exchangers (or part of the ground heat storage as in 30° sector model shown in Fig. 2). Strong advantages of 0D model compared to the 1D model are simplicity and simulation speed.

## 6.2. Mathematical and numerical 0D model

The governing equation for the heat transfer in the rock is a simple transient heat conduction equation with constant coefficients:

$$\rho_R C_{pR} \frac{\partial T_R}{\partial t} = \lambda_R \nabla^2 T_R \quad (1)$$

where  $T_R$ ,  $\rho_R$ ,  $C_{pR}$  and  $\lambda_R$  are temperature, density, specific heat at constant pressure and thermal conductivity of the rock. A convective heat transfer boundary condition is applied on the boundary in contact with the fluid:

$$-\lambda_R \nabla T_R \cdot \mathbf{n} = \Gamma (T - T_R) \quad (2)$$

where  $T$  and  $\Gamma$  are fluid temperature and heat transfer coefficient, respectively and  $\mathbf{n}$  is the outward pointing normal. The heat transfer coefficient is computed using the correlations proposed by Kirillov et al. for heating and cooling (during discharge and charge) of supercritical fluids [9] in mixed convection regime:

$$\Gamma = \Gamma(Re, Gr, Pr, T_{wall}) \quad (3)$$

For each exchanger, the global mass and energy conservation equations are:

$$\frac{d\rho}{dt} \forall + (G_{out} - G_{in}) = 0 \quad (4)$$

$$\frac{d(\rho h)}{dt} \forall + (G_{out} h_{out} - G_{in} h_{in}) = Q \quad (5)$$

where  $\rho$  and  $h$  are fluid density and enthalpy, respectively.  $\forall$  is the fluid volume (including the fluid contained in both annular and circular pipe),  $Q$  is the power transferred from/to the rock and  $G$  is the mass flow rate. Fluid density and temperature are computed as a function enthalpy and pressure:  $\rho = \rho(h, p)$  and  $T = T(h, p)$ . Please note that the momentum balance equation simply reduces to a pressure drop equation; this equation has been neglected since the overall pressure drop is sensibly smaller than the absolute pressure. As a consequence the fluid pressure can be reasonably assumed to be the same for all the exchangers. Of course it is possible to compute the fluid pressure by solving a pressure drop equation for each exchanger thus taking into account the small distributed head



losses as well as the localized ones. The total power transferred to/from the fluid is computed integrating the local power over the fluid-rock surface:

$$Q = \int_S \Gamma (T_r - T) dS \quad (6)$$

Finally one hypothesis on the outlet enthalpy  $h_{out}$  must be introduced: its effect on the accuracy of the 0D model is very significant. The difference of results with the mentioned 1D model would indeed be quite large if we simply assume  $h_{out} = h$ , while it can be minimized if we compute  $h_{out}$  assuming a quadratic interpolation based on  $h_{in}$ ,  $h$  and the enthalpy of the next exchanger:

$$h_{out}(i) = -\frac{1}{3}h_{in}(i) + h(i) + \frac{1}{3}h(i+1) \quad (7)$$

The mathematical model was implemented in OpenFOAM® [10]; equation (1) was discretized using a second-order accurate finite volume method. The rock is assumed to be granite (see Table 2 for granite thermo-physical properties). The thermodynamic and transport properties of carbon dioxide are computed using the CoolProp library [11]. The above-mentioned non-linear ODEs can be solved either implicitly or explicitly. While both methods have been implemented, the explicit solution was finally chosen due to its simplicity and since it proved to be faster. The most important steps of the explicit solution algorithm are described hereinafter. For a given exchanger we start by solving explicitly equation (5), thus computing  $h$ . Then  $\rho$  is updated using the equation of state and  $G_{out}$  is computed from equation (4). At this point we compute  $h_{out}$  as well as a residual criteria based on either  $h$  or  $h_{out}$  used to check whether convergence is achieved (residual < 1e-6). This iterative loop is required to ensure that both mass and energy conservation are simultaneously satisfied. This is repeated sequentially for each exchanger so that the governing equations are solved from the first to the last exchanger of a series (following the flow direction), thus properly updating inlet enthalpy and mass flow rate for each exchanger (set to the outlet values of the previous exchanger). Finally the heat equation is solved thus computing the rock temperature. The latter will be used at the next time-step to compute  $Q$ . Concerning the ODEs both 1<sup>st</sup> order (Euler) and 2<sup>nd</sup> order (RK2) methods have been tested for time discretization obtaining similar results.

### 6.3. Simulations and results of 0D model

The 0D model described in the previous section, as well as the 1D model presented in [8], have been used for performing a preliminary optimization of the ground heat storage. The objective was to increase the exergy efficiency  $\eta_{ex}$  computed based on the total amount of CO<sub>2</sub> exergy extracted from/sent in the storage:

$$\eta_{ex} = (Ex_{out} - Ex_{in})_{\text{discharge}} / (Ex_{in} - Ex_{out})_{\text{charge}} \quad (8)$$

This value gives an estimation of what would be the overall electrical efficiency of the storage system if we had ideal Carnot engines to produce heat (during charge) and electricity (during discharge). During the optimization some parameters have been fixed, in particular: number of exchangers in the series ( $n = 45$ ), CO<sub>2</sub> inlet temperature and pressure during charge (411.15 K and 12 MPa) and discharge (303.15 K and 12 MPa) for the series of exchangers. The initial simulation considered 5 cycles with 6 h charge / 6 h discharge,  $G = 4$  kg/s and 12 m long exchangers. The simulation shows that in these conditions the effects of convection are simply too strong and, as a result, the exergy efficiency  $\eta_{ex}$  is low (47%). Increasing the exchangers' length, reducing the mass flow rate and using different flow rates during charge and discharge allowed us to increase the exergy efficiency. In the "optimized" configuration we considered: 6 h charge with  $G = 1.75$  kg/s and 4h discharge with  $G = 2.5$  kg/s, 30 m long exchangers (note that 18 cycles have been modeled). Some results of this simulation are shown in



Fig. 3–4. After 6 cycles the exergy efficiency is higher than 65% and it reaches a quasi-steady value of  $\sim 75\%$  after 12 cycles. The simulations also show that the errors introduced using the 0D model are small ( $<1$  K), provided that the above mentioned quadratic interpolation is employed for computing  $h_{out}$  (see Fig. 4b).

## 7. Heat exchanger prototype 1/10 scale

Motivation of the experimental project bench set up by SeleCO<sub>2</sub> project at CEA (Grenoble) is to investigate on 1/10 scale heat exchanger prototype the heat transfer performance and the storage dynamics. The working fluid is sCO<sub>2</sub> circulating inside a vertical coaxial heat exchanger. A granite column is axial drilled to accommodate at center the heat exchanger prototype. Results are also intended to validate the conjugate heat transfer CFD simulations of a single exchanger. Heat exchanger prototype is 33 mm diameter (DN25), 1.6 m long and made of 316 Stainless Steel. Granite column is 100 mm diameter, 1.6 m long. Thermal coupling between heat exchanger prototype and granite column is done using thermal grease. Maximum temperature ( $\sim 130^\circ\text{C}$ ) and pressure ( $\sim 120$  bar) conditions of the working fluid on the bench are similar to the operating conditions of the SeleCO<sub>2</sub> process.

Experiments are conducted to investigate different temperatures and mass-flow rates for the working fluid in charge/discharge cycles. There is however some inherent limitation for such reduced scale model: the flow regime of sCO<sub>2</sub> inside the heat exchanger prototype ( $\text{Re} \sim 10^4$ ) remains still far from the flow regime in the full-scale geothermal heat exchanger ( $\text{Re} \sim 10^6$ ). First experimental results of prototype show that energetic and exegetic performances are better if a short charge and discharge strategy is chosen rather than a long charge followed by discharge cycles.

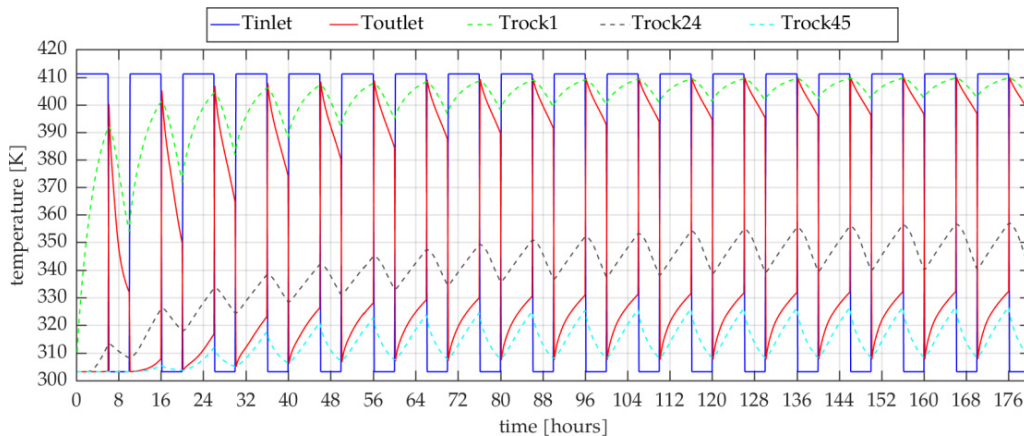


Fig. 3. Temporal evolution of inlet and outlet temperature for a series of exchangers (continuous lines) and volume-averaged rock temperature for 1<sup>st</sup>, 24<sup>th</sup> and 45<sup>th</sup> exchanger (dashed lines).

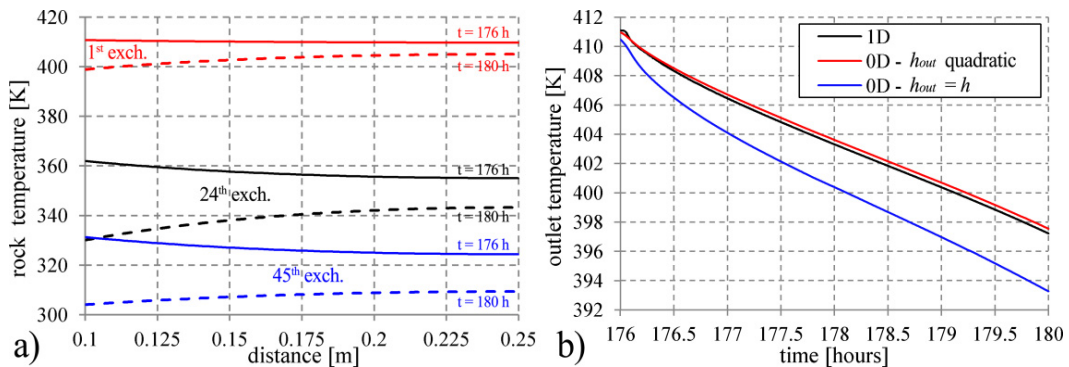


Fig. 4. (a) Rock temperature radial profile next to 1<sup>st</sup>, 24<sup>th</sup> and 45<sup>th</sup> exchanger at the end of the last charge (176 h) and at the end of last discharge (180 h); (b) comparison 0D and 1D model – temporal evolution of outlet temperature during last discharge.

## Acknowledgements

The authors acknowledge the support of the French National Research Agency (ANR) under grant ANR-13-SEED-0004 (SeleCO2 project). Project partners are ENGIE, BRGM, CEA, Enertime and IMFT.

## References

- [1] ENEA Consulting. Facts & Figures: Le Stockage d'Energie, 2012.
- [2] M. Mercangöz, J. Hemrle, L. Kaufmann, A. Z'Graggen, C. Ohler, Electrothermal energy storage with transcritical CO<sub>2</sub> cycles, *Energy* 45 (2012) 407–415.
- [3] J. Hemrle, L. Kaufmann, M. Mercangoez, Thermoelectric energy storage system having two thermal baths and method for storing thermoelectric energy, Patent EP2241737 (2009).
- [4] T. Desrues, J. Ruer, P. Marty, J.F. Fourmigué, A thermal energy storage process for large scale electric applications, *Applied Thermal Engineering*, 30 (2010), 425–432.
- [5] F. Ayachi, N. Tauveron, T. Tartièrre, S. Colasson, D. Nguyen, Thermo-Electric Energy Storage involving CO<sub>2</sub> transcritical cycles and ground heat storage, *Applied Thermal Engineering*, 108 (2016) 1418–1428.
- [6] J.P. Von Eller, J.G. Blanalt, B. Pfeiffer, Geological Map of France to 1/50000, Saint-Dié geological map (306) (in French), BRGM (1975).
- [7] R. Houpert, F. Homand-Etienne, Mechanical behavior of rocks as a function of temperature (in French), *French Geotechnical Journal* 28 (1984) 41–47.
- [8] E.G. Macchi, C. Colin, T. Tartièrre, D. Nguyen, N. Tauveron, Thermoelectric energy storage based on CO<sub>2</sub> transcritical cycles: ground heat storage modelling, 1st European Seminar on Supercritical CO<sub>2</sub> Power Systems (2016).
- [9] I.L. Pioro, H.F. Khartabil, R.B. Duffey, Heat transfer to supercritical fluids flowing in channels – empirical correlations (survey), *Nucl. Eng. Des.* 230 (2014) 69–91.
- [10] H.G. Weller, G. Tabor, H. Jasak, C. Fureby, A Tensorial Approach to Computational Continuum Mechanics using Object-Oriented Techniques, *Comput. Phys.* 12 (1998) 620–631.
- [11] I.H. Bell, J. Wronski, S. Quoilin and V. Lemort, Pure and Pseudo-pure Fluid Thermophysical Property Evaluation and the Open-Source Thermophysical Property Library CoolProp, *Ind. Eng. Chem. Res.* 53 (2014) 2498–2508.